Ceramics International 49 (2023) 24487–24498

Contents lists available at ScienceDirect

Ceramics International

journal homepage: www.elsevier.com/locate/ceramint

Prospects for industrial vanadium flow batteries

Andrea Trovò [a,b], Matteo Rugna [a,b], Nicola Poli [a,b], Massimo Guarnieri [a,b,*]

[a] Department of Industrial Engineering – University of Padua, Padova, Italy
[b] Interdepartmental Centre Giorgio Levi Cases for Energy Economics and Technology, University of Padua, Padova, Italy

ARTICLE INFO

Handling Editor: Dr P. Vincenzini

Keywords:
Renewable energy
Energy storage
Electrochemical energy storage
Flow batteries
Vanadium flow batteries

ABSTRACT

Vanadium Flow Batteries (VFBs) are a stationary energy storage technology, that can play a pivotal role in the integration of renewable sources into the electrical grid, thanks to unique advantages like power and energy independent sizing, no risk of explosion or fire and extremely long operating life. The first part of this paper presents the main features and the basic performance parameters of VFB, which determine their electric, hydraulic, thermal, and aging feature. The latter part outlines the strengths and weaknesses of the technology, the services that it can provide to the grid, and a short economic analysis. After presenting the fundaments of the technology, prospects and trends of VFBs deployment are outlined. Most of the considerations highlighted in this paper are inspired to studies performed on an industrial-size VFB operated at the Electrochemical Energy Storage and Conversion Lab (EESCoLab) at the University of Padua (Italy).

1. Introduction

1.1. Energy storage

In the last decades, the burn of fossil fuels for energy production and vehicles propulsion has had an increasing environmental impact. To mitigate climate change, the growing demand for energy needs to be fulfilled with decarbonized and environmentally friendly renewable energy sources (RESs), and this transition has already been started, driven by long-term governmental programs aiming at abandon fossil fuels by 2050. Unlike conventional power plants, renewable sources such as wind turbines and solar panels do not generate electricity on demand, but according to weather and astronomical conditions, which creates a mismatch between power offer and demand such that a renewable source production share of 20% may be sufficient to destabilize the grids, resulting in black-outs and supply halts [1]. A pivotal solution to this issue consists in energy storage (ES) of surplus production in low demand period and its release in high demand periods. For a reliable integration into the grid, a storage technology must be technically and economically competitive, namely it must ensure sufficient storage capacity, withstand a high number of charge/discharge cycles, provide flexible and safe operation, and present low capital investment and operative costs. ES systems are required to provide different services to the grid: depending on the operating and response time, the services can be divided in power quality and energy management. The former includes operations on the short timescale (ms - min), like frequency regulation, voltage sag compensation, power smoothing and grid stabilization. The latter refers to operations on a longer timescale (min - h) as load leveling, peak shaving, time shifting and UPS (uninterruptable power supply) [2]. Every storage technology has its own features, which place it in a different position of the power duration/diagram (Fig. 1): Pumped hydro energy storage (PHES) [3], compressed air energy storage (CAE) [4], and thermal energy storage (TES) [5] are suitable for long-duration applications (several hours), conversely flywheel energy storage (FES) [6], superconducting magnetic energy storage (SMES) [7] and electric double layer capacitor (EDLC) [8] can guarantee a very fast response, on a second–minute timescale [9].

Electrochemical Energy Storage (ECES) can be used for both fast response and intra-day applications, covering an area of the diagram that is not occupied by other technologies. Unlike PHES and CAE, ECES benefits of site versatility because it does not require specific territory features. Furthermore, modularity and absence of moving parts allow wide scalability, ease of use and low maintenance, making ECES extremely suitable for the development of RES-based grids.

1.2. Flow batteries

Among ECES technologies, Lithium-Ion Batteries (LIBs) are the most widespread. However, LIBs present some limitations: energy and power are bonded together by the internal chemistry so that they are not suitable for discharges longer than 4 h, their life hardly extend beyond

* Corresponding author. Department of Industrial Engineering – University of Padua, Padova, Italy.
E-mail address: massimo.guarnieri@unipd.it (M. Guarnieri).

https://doi.org/10.1016/j.ceramint.2023.01.165
Received 28 September 2022; Received in revised form 22 December 2022; Accepted 24 January 2023
Available online 25 January 2023

Nomenclature

Full names

Ac	Active area
ASR	Area specific resistance
BMS	Battery management system
BP	Bipolar Plate
Cv	Vanadium concentration
CAE	Compressed air energy storage
CAPEX	Capital expenditures
CCF	Cumulative cash flow
DICP-RKP	Dalian Institute of Chemical Physics – Rongke Power
DOE	Department of Energy
ECES	Electrochemical energy storage
EDLC	Electric double layer capacitor
EIS	Electrochemical impedance spectroscopy
ESS	Energy storage system
F	Faraday constant
FB	Flow battery
FES	Flywheel energy storage
FF	Flow frames
HESS	Hydrogen energy storage system
IS-VRFB	Industrial scale - vanadium flow battery
jc	Current density
LCOS	Livelized cost of storage
LIB	Lithium ion batteries
MEA	Membrane electrode assembly
Nc	Number of cells in a single stack
NPV	Net present value
OCV	Open circuit voltage
P	Electrical power
Pp	Pumping power
Ph	Hydraulic pumping power losses
PCS	Power conditioning system
PEM	Proton exchange membrane
PEMFC	Proton exchange membrane fuel cell
PHES	Pumped hydro energy storage
Q	Flow rate
RES	Renewable energy sources
TES	Thermal energy storage
SHE	Standard hydrogen electrode
SMES	Superconductive magnetic energy storage
SOC	State of Charge
SOH	State of Health
UPS	Uninterruptible power supply
VFB	Vanadium flow batteries
α	Flow factor
Δp	Pressure drops of the hydraulic circuit
Δp_s	Pressure drop inside the stack
Δp_{pi}	Pressure drop inside the piping
Q	Flow rate
Qs	Stack flow rate
Vs	Stack voltage
ηa	Activation overpotential
ηan	Overall ancillary efficiency
ηc	Concentration overpotential
ηo	Ohmic overpotential

5000 cycles after which a major loss in capacity occurs, risks of fire and explosions exists (and persist also when advanced safety systems are installed), and issues in raw materials supply rise concerns when the coming forecasted expansion of the demand in the next years is considered.

Among ECES systems for stationary applications, a highly promising technology consists in Flow Batteries (FBs), which in recent years have expanded their commercial availability. FBs use liquid electrolytes which are stored in two tanks, one for the positive electrolyte (catholyte) and the other for the negative one (anolyte), as shown in Fig. 2. During charge and discharge, the electrolytes are cycled inside of an electrochemical reactor (called "stack") made of several cells where, flowing within the cell porous electrodes, they undergo electrochemical reactions which convert chemical energy into electrical energy and vice versa. This design uncouples power and energy, which is not possible for conventional closed ECES systems like LIBs. The possibility of decoupling power and energy can guarantee long discharge time and the chance of using FBs not only as grid buffer but also in other application like support of charging station for EVs. The *All-Vanadium* type is the most developed FB, due to its good power and energy densities, good

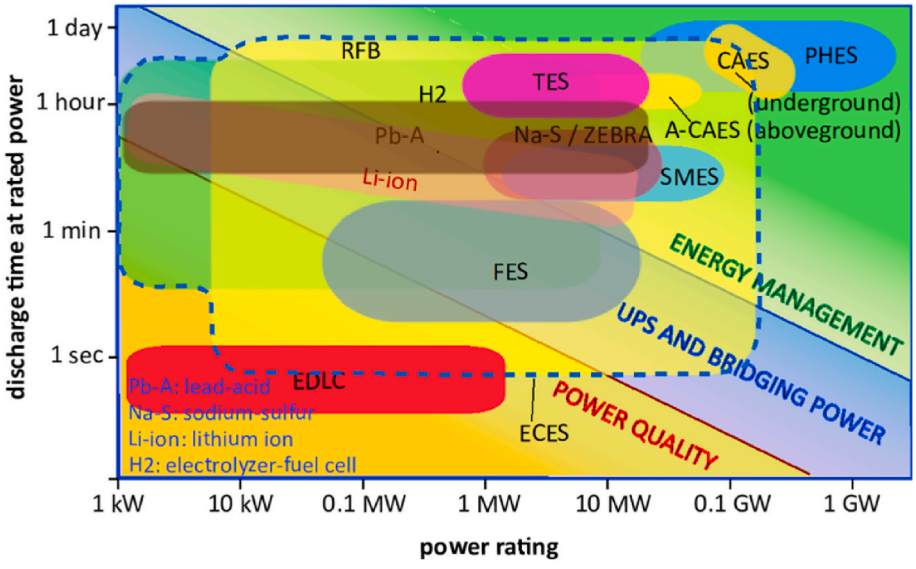

Fig. 1. Ragone-like plot of energy storage systems.

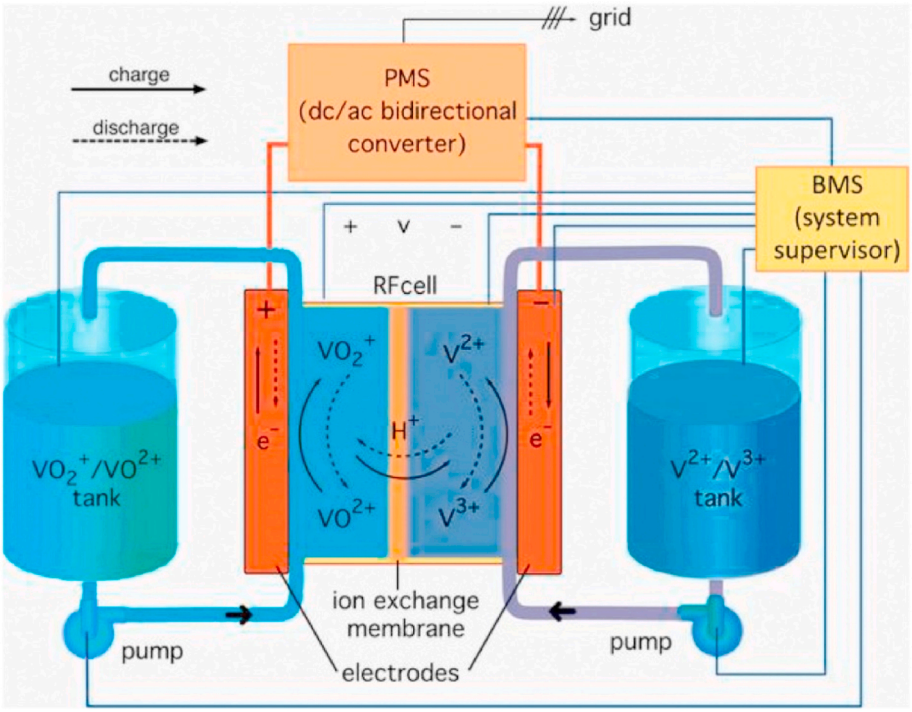

Fig. 2. A vanadium flow battery scheme. Pumps move the liquid electrolytes from the tanks to the stack where the redox reactions take place (courtesy of Elsevier J Power Sources [9]).

efficiency, and very long life [10]. Currently, the Chinese DICP-RKP (Dalian Institute of Chemical Physics – Rongke Power) group is working on the 200MW/800 MWh all-vanadium FB (VFB), which will be a world-top ECES facility [11]. In addition to all-fluid FBs, there are systems with solid electroactive materials deposited inside the stack, called hybrid FBs (e.g. zinc-bromine FBs), whose commercial diffusion is much lower than VFBs.

A vanadium flow battery uses electrolytes made of a water solution of sulfuric acid in which vanadium ions are dissolved. It exploits the ability of vanadium to exist in four different oxidation states: a tank stores the negative electrolyte (anolyte or negolyte) containing V(II) (bivalent V^{2+}) and V(III) (trivalent V^{3+}), while the other tank stores the positive electrolyte (catholyte or posolyte) containing V(IV) (tetravalent VO^{2+}) and V(V) (pentavalent VO_2^+). In commercial VFBs, to avoid precipitations the electrolyte concentration ranges between 2 and 5 mol L^{-1} for the sulfuric acid and 1.5–2 mol L^{-1} for the vanadium ions. With such vanadium concentration the energy density of VFBs is between 20 and 30 Wh L^{-1}. Laboratory tests have shown that a significant enhancement in the energy density of the electrolyte can be achieved by using additives that act as precipitation inhibitors for the vanadium ions at concentrations of 2.2–2.5 mol L^{-1} [12]. The electrochemical half-reactions that occur in the cells are.

Positive electrode

$$VO_2^+ + 2H^+ + e^- \underset{\text{charge}}{\overset{\text{discharge}}{\rightleftharpoons}} VO^{2+} + H_2O \quad E_{0+} = +1.00\ \text{V} \quad \text{vs. SHE} \tag{1}$$

Negative electrode

$$V^{2+} \underset{\text{charge}}{\overset{\text{discharge}}{\rightleftharpoons}} V^{3+} + e^- \qquad E_{0-} = -0.26\ \text{V} \quad \text{vs. SHE} \tag{2}$$

The corresponding Open Circuit Voltage (OCV) of the cell is E_0 = 1.26 V at standard conditions T = 298.15 K and SOC = 50%. Real cells exhibit E_0' = 1.4 V due to side effects such as the Donnan potential [13].

Like fuel cells (FCs), the electrochemical reactor of a VFB is a stack of several cells connected electrically in series and fed hydraulically in parallel. Each cell includes two carbon-based porous electrodes (e.g. carbon felt, carbon-fiber paper, or carbon nanotubes) which, in operation, are flooded by the electrolytes. The electrodes are separated by an ion-exchange polymeric membrane that keep separated the positive and negative electrolytes as shown in Fig. 3a. It allows balancing ions passing from one to the other electrode to maintain the electrical neutrality of the system and, at the same time, since the electrons cannot cross the membrane, they flow in the external circuit, consuming/releasing electrical power from/to the grid. To ensure both electric and hydraulic connections, the cells are interleaved with flow frames (FF) encasing conducting plates, called bipolar plates (BPs), which ensure the electrical connections between adjacent cells while separating the solutions of opposite polarity (Fig. 3b) [14].

2. Characterization and development of a VFB

The development of a high–performance VFB cannot exclude tests on small single cell devices for the characterization of active materials and tests on large area multiple-cell stacks for the assessment of the electrical, thermal, and hydraulic performance of the battery. In the following paragraphs the main features of a VFB will be presented together with some recent results obtained at the Electrochemical Energy Storage and Conversion Laboratory (EESCoLab) of the University of Padua (Italy), where an Industrial Scale Vanadium Redox Flow Battery (IS-VRFB) is used as a base for kW-class studies [14]. Pilot plants like the IS-VRFB allow to highlight critical issues of a real system, which represents a challenge in the production of resilient and efficient commercial FBs.

2.1. Electrical characterization

The electric power of the battery is related to the size of the stack. The cell voltage depends on the current density, i.e. the cell polarization curve, can be modeled with the following equation:

$$V_c = OCV - \eta_a - \eta_c - \eta_o = OCV - ASR\, j_c \tag{3}$$

Where OCV ≈ E_0' is the Open Circuit Voltage, ASR is the Area Specific

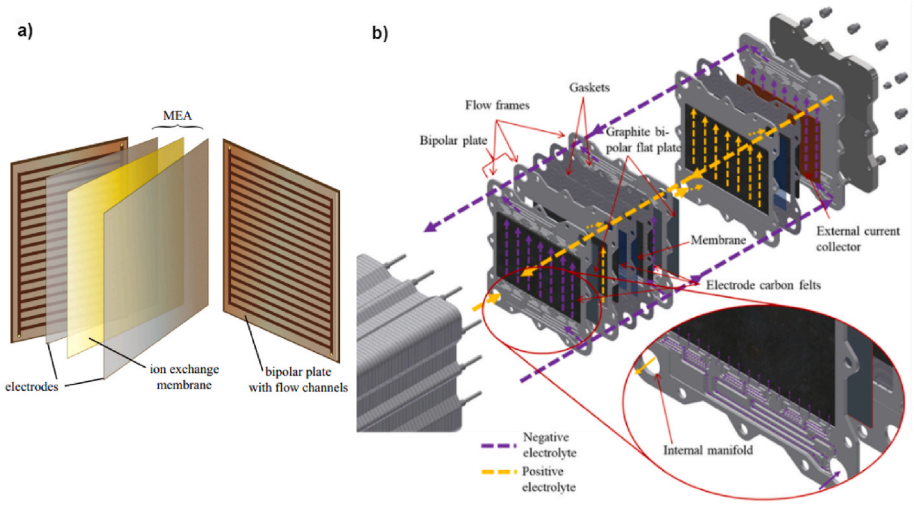

Fig. 3. (a) MEA (membrane-electrode assembly) and bipolar plates of a PEMFC. (b) Cell and stack configuration of the IS – VRFB studied at the EESCoLab of the University of Padua (Italy) (courtesy of Elsevier Appl Energy [14]).

Resistance and j_c is the current density (with the convention that $j_c > 0$ in discharge and $j_c < 0$ in charge). ASR is a synthetic parameter related to the internal resistance R as $R = ASR/A$, with A the cell active area. It takes into account cell effects such as the activation η_a and concentration η_c overpotentials in the electrodes and the electrical conductivity associated with membrane, electrodes, bipolar plates, electrolytes and their interfaces, which are counted as ohmic overpotential η_o. Both OCV and ASR vary with the battery State Of Charge (SOC). Small-scale single cell tests are typically performed for characterizing the cell active materials, namely membrane [15–18], electrodes [19–21], current collectors [22] and bipolar plates [23–25], for identifying which material combination minimizes the ASR [26].

Since V_c has to be kept within a specific range, i.e. between ≈1 V (in discharge) and ≈1.6 V (in charge), j_c must be kept among a specific interval in charge and another in discharge, according to the SOC condition, as shown in Fig. 4a. When these values are determined, the cell active area A_c can be chosen to achieve power requirements, as follow:

$$A_c = \frac{P}{j_c\, E_c\, N_c} \tag{4}$$

Where P is the rated electrical power and N_c is the number of cells forming the stack. This latter is usually in a range of 40–50 cells, which is a trade-off between a high stack voltage to ease electric power management in the power conditioning system (PCS) interfacing the battery to the grid and low "shunt currents", i.e. the parasitic currents flowing in the electrolytes from one cell to the next due to the electrolyte conductivity (see Section 2.3). Typically, A_c is evaluated in the most critical conditions, namely at SOC as low as 10% in discharge and as high as 90% in charge. The largest between the resulting two values is adopted.

Similar measurements are performed on stacks made of several large cells. An example of electrical characterization on a VFB system is reported in Ref. [27], which consider an industrial-size 9 kW/26 kWh, 40-cells 600-cm^2 stack (IS-VRFB). The obtained polarization curves during charge and discharge, in two cases are reported: the former pertains to fast response applications in a timescale of few seconds which can be of interest in *power quality* services such as frequency regulations, the latter pertains steady state operating conditions which can be of interested in *energy management* services such as peak shaving. Families of polarization and power curves as function of SOC and flow rate Q were obtained (Fig. 4a and b). These data provide information on the internal resistance of the stack and on the maximum current density (higher than 600 mA/cm^2). Another interesting result is presented in Fig. 4c, where the power curves, at a constant SOC = 70%, are plotted at some flow rate Q, showing that the maximum power varies with Q. This means that the delivered power can be maintained constant while the SOC changes by modulating Q. The testing procedure presented in Ref. [27] can constitute a standard approach for the performance assessment of kW-class VFBs, which at present is lacking, and can contribute to the definition of performance parameters for the comparison of different *All-vanadium* redox flow batteries [28]. To analyze

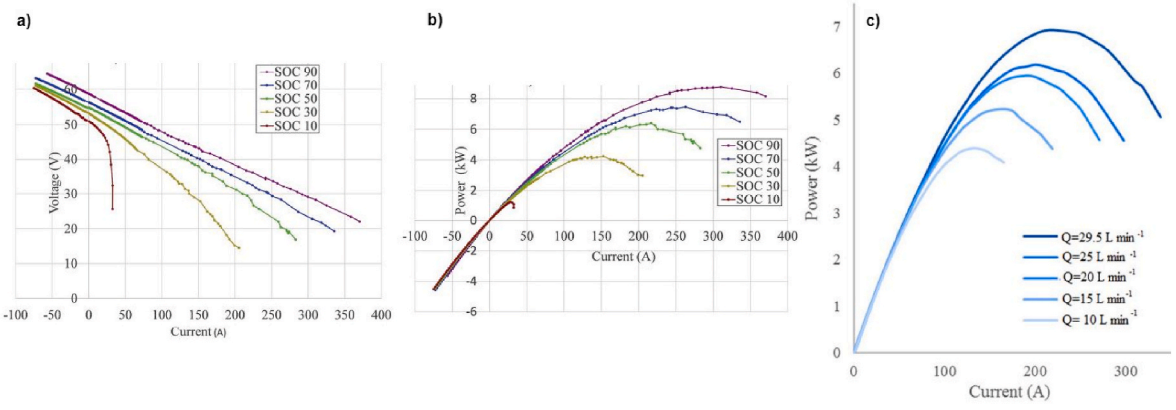

Fig. 4. a) Polarization curves for fast response at different SOCs with $Q = 29.5$ Lmin^{-1}; b) Power curves at different SOCs with $Q = 29.5$ Lmin^{-1}; c) Discharge power curve at SOC = 70% and different flow rates Q (courtesy of Elsevier J Power Sources [28]).

the performance of the battery, it is also necessary to evaluate the response characteristics of the stack, to design an effective power conditioning system (PCS), which interfaces the battery with the grid.

In an early study, two kW-class batteries were analyzed, in respect to the connection with a passive load (a resistor), and an electronic load operating in a galvanostatic mode [29]. During the experiment the batteries were discharged and the evolution of current and voltage was evaluated in two timescales: 20 ms and 120 s, corresponding to fast responses (of interest in quality services) and slow response (of interest in power management) applications. The discharge on a passive load revealed a time, of approximately 7 ms, characterized by a large swing in the stack current and voltage (Fig. 5). The absence of large fluctuation during the discharge through the power electronics interface proves that VFBs can ensure quality services to the grid if properly driven by the PCS. This result is important because millisecond response time is a prerequisite to provide frequency regulation for the grid. The experimental data obtained by the 120 s analysis, revealed insertion overcurrents up to 130% and overpowers up to 160% (Fig. 6). To complete the investigation on the long timescale, a numerical simulation on an equivalent electrical circuit, representing the battery discharge, was computed for different SOC, *Q*, load and discharge mode. As opposed to the experimental results, the simulation was characterized by the absence of fluctuations, demonstrating that current and voltage swings are caused by electrochemical phenomena, like successive activations of different vanadium species occurring at the solid-electrolyte interfaces in the positive electrode, due to the varying accumulation of different vanadium complexes.

2.2. Thermal characterization

The operating temperature of a VFB may vary due to cell dissipative effects related to electrical resistance, electrochemical reactions, and environmental condition, thus affecting electrode kinetics, transport property and ohmic resistance [30]. Zangh et al. report a higher battery voltage efficiency and an improved peak power density when the temperature increases from 15 °C to 55 °C, together with a lower energy consumption from the pumps related to a lower viscosity of the electrolytes [31]. However, undesired side effects tend to increase at high temperature, like hydrogen and oxygen evolutions and vanadium ions crossover through the membrane, causing a lower coulombic efficiency and capacity decay [32,33]. In addition, several studies have focused their attention on vanadium precipitations in the electrolytes at high temperature, which reduces the storage capacity, the pump reliability and the stack performance. Usually, V(II), V(III), and V(IV) precipitate at low temperature (e.g. V(IV) at a concentration of 2.0 M VO^{2+}/5.0 M H_2SO_4 reaches its solubility limit below −5 °C [34]), while V(V), for concentration of about 2.0 M, precipitate after few days when it is kept at a temperature above 40 °C [35]. To increase the energy capacity of the battery, high vanadium ions concentrations can be reached by mixing the electrolyte with sulfate–chloride [36] or with organic and inorganic chemicals additives [37,38]. So far, an operating temperature in the range of 10 °C–40 °C is considered safe in most commercial applications. Since the electrolyte stored in the tanks keeps isothermal with the room, which is controlled by an air conditioning system, even if the temperature inside the stack increases during operations, the electrolytes flow removes the heat, providing an effective cooling. Differently, the thermal behavior of a VFB stack in standby condition cannot rely on such cooling when power and reactant flow are turned off. In this condition the temperature inside the cells increases because of Joule effects produced by shunt currents and side reactions between vanadium species, occurring after unavoidable species crossover through the membrane. Trovò et al. presented a numerical dynamic model of cells temperature evolution during standby conditions [39]. The study demonstrates that at high SOC the cells are subjected to an increase in temperature up to 10 °C, which can trigger VO_2^+ precipitations. To avoid internal heat generation in no-load conditions, the stack can be emptied, so that no side reactions and consequently no self-discharge occur. However, in this way is no more possible to ensure fast grid services (e.g. frequency regulation) because filling the stack and bringing it up to a ready state require too much time. Conversely, a strategy for ready-to-operate standby conditions may consist in applying a constant small flow rate of "cold" electrolyte, but this implies additional energy losses. A different strategy may consist in an advance cooling protocol to keep the temperature within safety limits while minimizing additional losses. The IS-VRFB was provided with such a standby thermal management system, capable of performing two different standby modes: *swamped standby mode,* characterized by smart intermittent washings and *streamed standby mode,* that provide a small electrolyte cooling flow rate [40]. Fig. 7 shows that the electrolyte that fill the stack, if not removed, increases its temperature with a peak that raises with the SOC of the battery. The *swamped standby mode* was able to minimize self-discharge losses to 1.9% of the nominal charge capacity over a standby duration of 1.5 h, while the *streamed standby mode* exhibited a self-discharge of 10.5% over a standby period of 6 h. The former mode

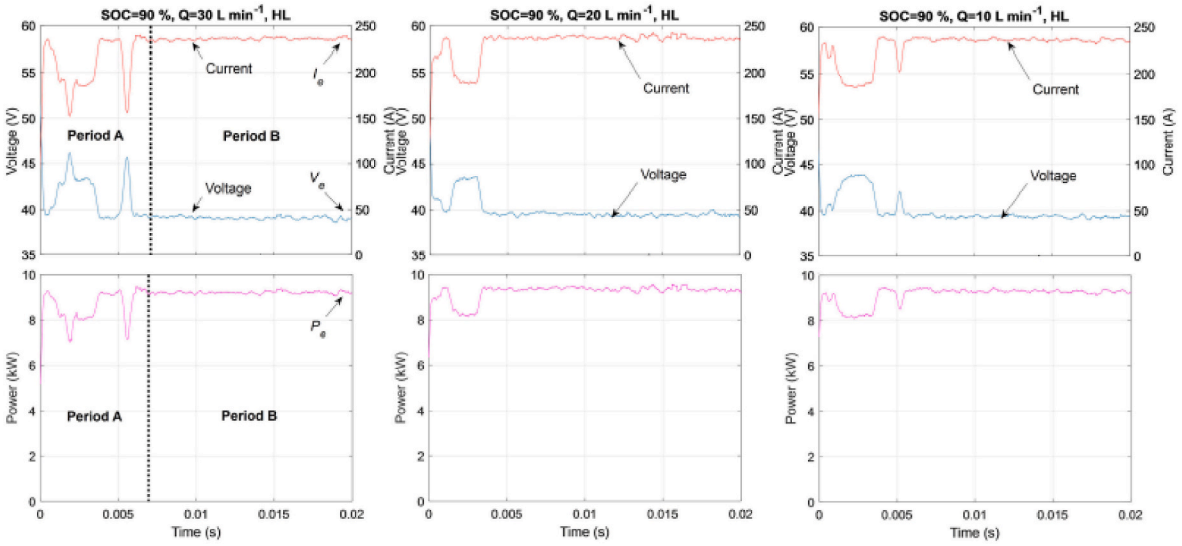

Fig. 5. Measured IS-VRFB current, voltage and power in the early 20 ms of discharges on a passive load, at SOC = 90% and for different flow rate *Q* (courtesy of IEEE Trans Sustain Energy [29]).

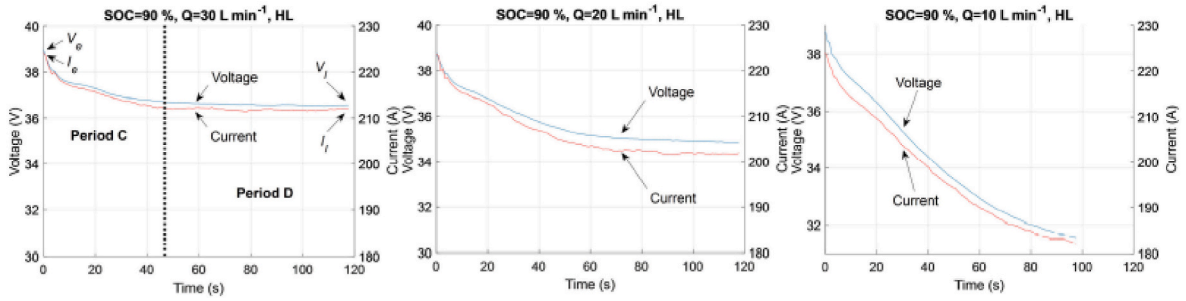

Fig. 6. Measured IS-VRFB current and voltage in the early 120 s of discharges on a passive load, for $Q = 30/20/10$ L/min, at SOC = 90% (courtesy of IEEE Trans Sustain Energy [29]).

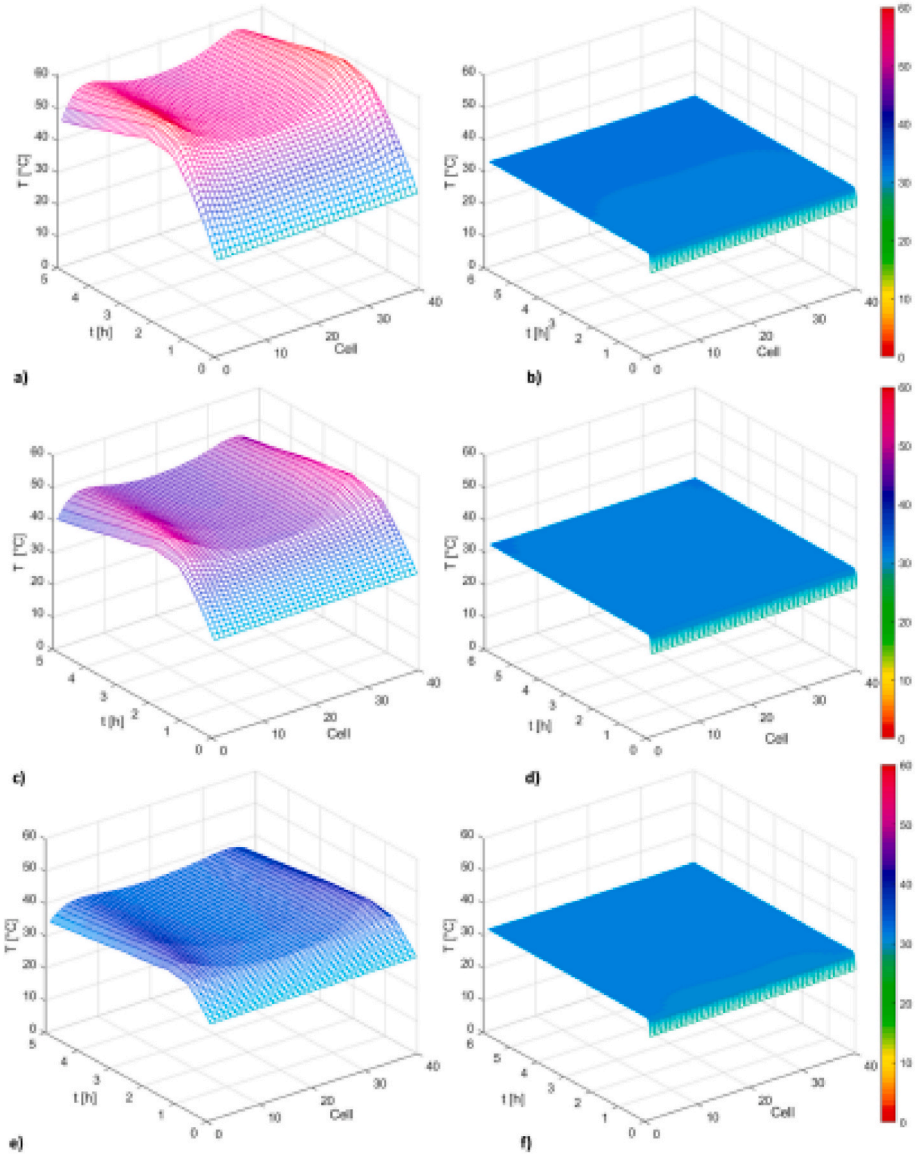

Fig. 7. Temperature distribution of the IS-VRFB, located at the EESCoLab (University of Padua), for swamped standby mode (a), (c), (e) and streamed standby mode (b), (d), (f) with an electrolyte flow rate $Q = 5$ L/min. The initial SOC of the battery is 95% for (a), (b); 65% for (c), (d); 20% for (e), (f). Initial temperatures are: $T_{air} = 25$ °C and $T_{stack} = 30$ °C (courtesy of Elsevier Energy Convers Manag [40]).

can be used in slow energy management services while the latter can be used in fast power quality services. This result may help to increase the life of the battery, avoiding vanadium precipitation and reducing self-discharge, leading to greater economic return.

2.3. Hydraulic characterization

In load operation, an electrolytes flow rate must be cycled in the stacks. In order to achieve the desired performance, the circulation

pumps must be chosen after estimating the pressure drops along the system and the electrolyte flow rate needed at rated electrical power [41]. The power P_p consumed by the pumping system consists of the hydraulic power losses in the piping P_h and the losses in the pumps, motors and feeding inverters, which can be accounted for in an overall ancillary efficiency η_{an}:

$$P_p = \frac{P_h}{\eta_{an}} \tag{5}$$

Where the net hydraulic power P_h can be expressed as follow:

$$P_h = Q_+ \Delta p_+ + Q_- \Delta p_- \tag{6}$$

Where $Q_\pm$ are the positive and negative electrolyte flow rates and $\Delta p_\pm$ are the pressure drops of the corresponding hydraulic circuit. The stack flowrates $Q_{S,\pm}$ depend on the battery electrical power P, on the vanadium concentration C_V, on the stack voltage Vs and on the flow factor α (the ratio between electrons available for the reaction and the fraction effectively reacting; typical α values are around 7–8). The stack flow rate during charge/discharge $Q_{c,S,\pm}/Q_{d,S,\pm}$ can be expressed as:

$$\begin{cases} Q_{c,S\pm} = \alpha \dfrac{N_c I}{F\, C_V (1 - SOC)} = \alpha \dfrac{P}{V_S\, F\, C_V (1 - SOC)} \\ Q_{d,S\pm} = \alpha \dfrac{N_c I}{F\, C_V SOC} = \alpha \dfrac{P}{V_S\, F\, C_V SOC} \end{cases} \tag{7}$$

where F is the Faraday constant. The pressure drops $\Delta p_\pm$ of the battery can be expressed as the sum of the pressure drop in the stack $\Delta p_{S,\pm}$ and in the piping $\Delta p_{pi,\pm}$:

$$\Delta p_\pm = \Delta p_{S,\pm} + \Delta p_{pi,\pm} \tag{8}$$

The hydraulic design must limit not only the pressure drops, but also the so-call *shunt currents*. Typically, the electrochemical cells, assembled into a stack, are electrically connected in series and hydraulically fed in parallel. Since the electrolyte is conductive, this configuration creates secondary paths through manifolds and channels where electric currents, called "shunt currents", flow, causing Joule losses affecting the battery efficiency. According to the literature [42], this loss reduces by ca.10% the energy efficiency of a VFB, both during its operation and in standby conditions. To reduce shunt currents, the electrical resistance of the hydraulic circuits need to be increased. The electrical resistance R of a segment of the hydraulic circuit depends on the electrolyte resistivity ρ and on its geometry. According to Ohm's law:

$$R = \rho \frac{l}{A} \tag{9}$$

Where l and A are the length and the cross-sectional area of the hydraulic circuit. In a VFB, ρ varies with the vanadium species concentrations and temperature. According to Ohm's law, it is possible to increase the electrical resistance by both reducing the section area and increasing the channels length. An analysis that takes into account all these factors is presented in Ref. [42]. From his study some general considerations can be extended to a wide range of kW-class VFBs. The major losses involved in a VFB systems are related to: cell overpotentials, species crossover, shunt currents, hydraulic pressure drops and power consumption due to ancillary devices (Fig. 8). Generally speaking, these losses do not impact equally on overall efficiency. In fact, in the case of IS-VRFB, shunt currents losses are tenfold to twentyfold higher than hydraulic losses and, as regards the membrane, the losses caused by the ion resistivity are higher than the losses caused by species crossover. Pumps and their motors, especially if small sized, can involve significant losses. What emerges from this analysis is that increasing the electrolyte electric resistances in the flow channels i.e. adopting long and thin flow channels inside the stack, is preferable in the trade -off between shunt current and hydraulic losses. As regards the energy efficiency, a membrane with a high ion conductivity is more important than one with reduced vanadium crossover.

2.4. Aging evaluation

Despite that VFBs can ensure 20 thousand charge and discharge cycles, this technology is not free from degradation mechanisms. Alongside the fundamental reactions of charge and discharge (1)–(2), some undesired side processes can occur: (i) oxidation of the V (II) ions in the negative half-cell as a consequence of air contamination, (ii) hydrogen evolution at the negative electrode, (iii) differential crossover of vanadium ions from one half-cell to the other, and (iv) volumetric transfer of an electrolyte from one half-cell to the other due to pressure difference [43]. Further degradation processes consist in the electrolyte precipitation, which reduce the capacity of the battery and may obstruct the pumps and the stack flow channels. Several methods can be used to overcome this problem. The easiest way to rebalance the electrolyte is a complete mixing of the positive and negative electrolytes stored in the two tanks. This mixing implies interrupting the operation of the battery, emptying the reservoirs and filling them again. To reduce the frequency of the conventional mixing procedure, tanks with anolyte and catholyte can be kept hydraulically connected by means of a bypass to ensure a natural redistribution of the two electrolytes [44]. However, this mixing technique is not effective against reductive and oxidative imbalances. Poli et al. tested a procedure for eliminating the charge imbalance caused by air-oxidation and hydrogen evolution, which is resorts to an electrolysis cell called "regeneration cell", where an electro-reduction reaction of V(V) is coupled with an oxygen evolution reaction catalyzed by a Ti – IrO_2 electrode [45]. The electrolyte is not the only

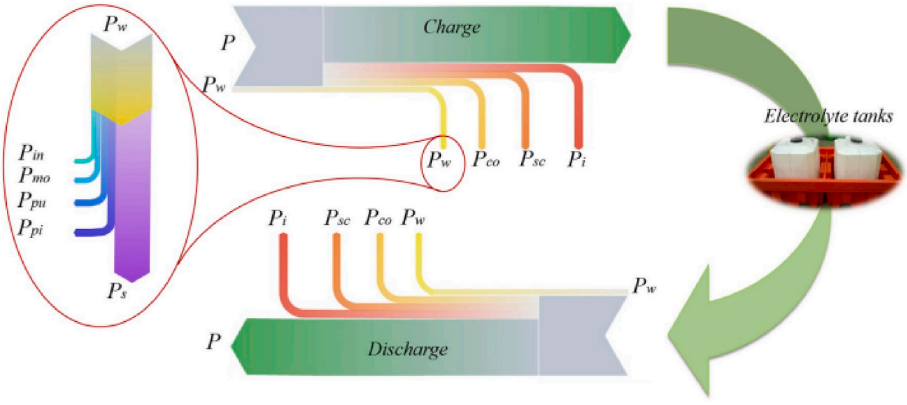

Fig. 8. Sankey diagram of the power flow of the IS – VRFB of the EESCoLab (University of Padua), with the impact of the power losses of the system on the overall energy efficiency of the battery (courtesy of Elsevier J Power Sources [42]).

element subjected to aging phenomena. Membranes degradation result in reduced capacity and increased ohmic losses. It can be related to chemical instability caused by high concentration of H_2SO_4 and by hydraulic pressure difference at both sides of the membrane, which leads to undesired transport of water and vanadium between the two cell electrodes, and, in the worst cases, it can cause its failure. Also, the carbon felt electrodes may be subjected to degradation due to chemical reaction with sulfuric acid and vanadium [46], furthermore, at high voltage (>1,65 V) the carbon can be oxidized with consequent CO_2 evolution. As concerns BPs, Kim et al. [47] advise that due to shunt currents the voltage between electrolyte and BPs increase, causing the electrolyzation of water. If water penetrates into the graphite bipolar plates may be electrolyzed and the generated gas may delaminate the graphite layer [25]. Materials with low degradation rate are the first step to amortize the initial investment in a longer period and make this technology more profitable. Since long-term stability tests are extremely time consuming, a solution can consist in the development of accelerated aging tests, performed with high temperature and high H_2SO_4 concentration.

An important tool to evaluate the State Of Health (SOH) of the active materials, i.e. the aging effect and any degradation phenomena that can occur during the lifetime of a VFB cell or stack, is the Electrochemical Impedance Spectroscopy (EIS). By means of an excitation sinusoidal signal at varying frequency, either current or voltage, electrochemical processes with a given characteristic time can be activated and each individual process contribution can be detected in a relatively short measurement time, such as: ohmic resistance, mass transport resistances and the interfacial charge-transfer resistance [48]. The sinusoidal stimulus is repeated sequentially at different frequencies in a range from 1 mHz to 1 MHz [48]. The response of the VFB cell or stack, in terms of voltage or current, allows to identify the impedance of the system, which characterizes its dynamic response, expressed in the frequency domain by means of Nyquist plots. From these plots, an equivalent electrical circuit model can be identified. A good equivalent circuit model consists of a dynamic Thevenin equivalent, which uses a voltage source and a combination of resistors, capacitors, and nonlinear elements. Examples of such equivalent circuits are shown in Fig. 9. Fitting the equivalent circuit to the experimental behavior of the EIS Nyquist plots provides the value of each equivalent circuit elements, which represents a specific process occurring inside the system. During the lifetime of the battery, the values of such elements may change, providing an indication of the aging of the system.

3. Key features: type of services, advantages and downside

3.1. Advantages

VFBs and other flow batteries can be sized independently in conversion power and energy storage. This feature, that FBs share with hydrogen energy storage systems (HESSs), allow for long discharge times without oversizing the stacks, resulting in commercial systems capable of delivering energy at full power for far more than 4 h, unlike other ECES systems such as lithium-ion battery, which at present are sold for discharge duration of 1–4 h. Since the positive and the negative electrolytes are stored in different tanks, no self-discharge occurs and VFBs can remain completely charged or discharged for long periods, like

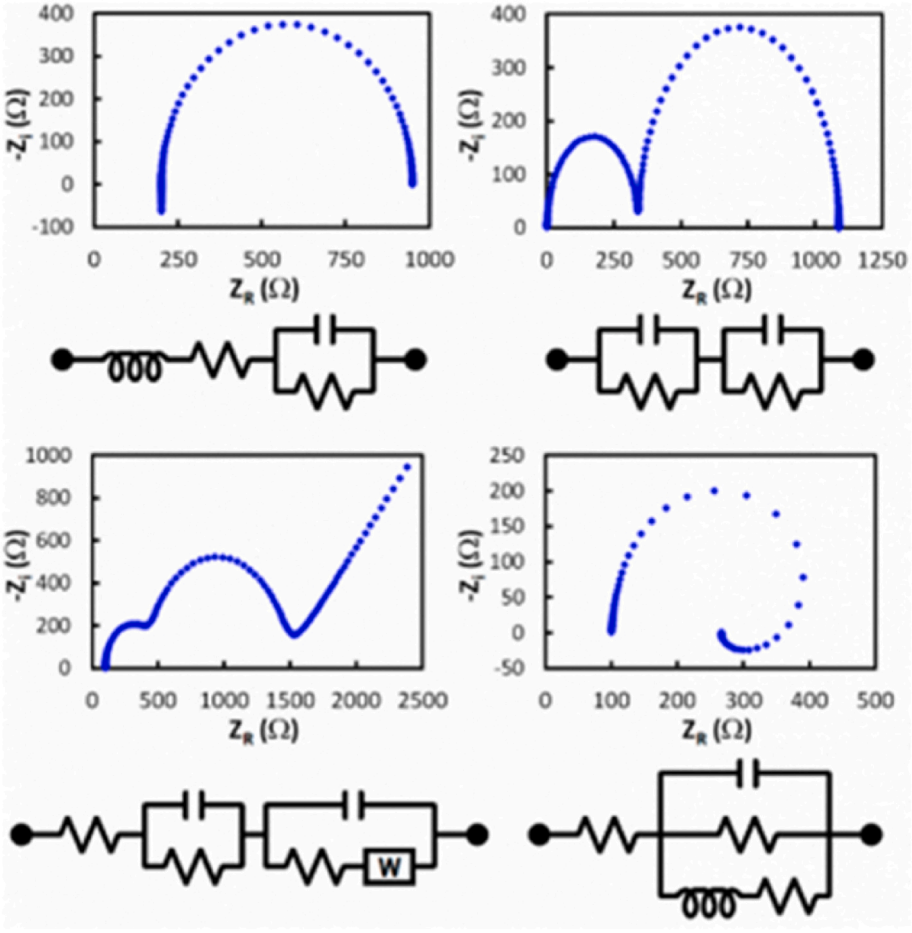

Fig. 9. Example of Nyquist plots and electrical circuit models used to simulate the electrical, chemical, and physical processes that occurs in a VFB system (courtesy of MDPI sensors [49]).

HESSs with Proton Exchange Membrane FC. However, VFBs present different advantages on HESSs. In fact, while HESSs, typically use an electrolyzer for the conversion of electricity into chemical energy of hydrogen and oxygen and a fuel cell for the opposite conversion, VFB reactors are completely reversible and perform both charge and discharge. In addition, HESS systems suffer from low round-trip efficiency and require high-pressure hydrogen storage, that implies losses and safety measures both of which are costly. VFBs operates by changing the oxidation states of the same metal at room temperature and pressure, with no risk of fire or explosion and by using low-cost tanks. The use of the same element, together with the absence of moving parts, allows for a long lifetime. Another advantage regards the low environmental impact. In fact, all the components of the battery are recyclable, and the electrolyte have extremely long lifetimes thanks to appropriate regeneration techniques [50]. At the end of the useful life of the plant, all electrolyte components (vanadium, water, and sulfuric acid) can be easily separated by precipitating electrochemically oxidized vanadium, resorting to pH change.

3.2. Drawbacks

The power and energy densities of VFBs, 100 W kg^{-1} and 20 Wh L^{-1} respectively, are low compared to other electrochemical devices. For this reason, to reach high power and energy value, cells with large area and reservoirs with high capacity (thousands of liters) are required, making them unusable in mobility applications. Another disadvantage is related to the shunt currents phenomenon, which takes place both during operation and standby reducing the SOC of the battery and affecting efficiency [51]. Even if the temperature it is not critical for safety, it must be controlled to avoid vanadium ions precipitation. Usually, a range of 10–40 °C is suitable for most applications as mentioned above. Another factor that can cause vanadium precipitation is the species crossover through the membrane that affects the ion solubility. Due to tanks, piping, pumps, sensors, controls, reactor structure, switch converter (PCS), and BMS, a VFB power plant is usually more complex than other ECES systems.

4. Economic evaluations

The CAPEX of a VFB includes the power component costs, the energy component costs and the costs needed for the assembly of the battery. The power component costs depend on the stacks sizes and therefore on the size of Flow Frame (FF), Bipolar Plate (BP), membrane, gasket, current collector and heads, while the energy component costs are mainly due to the electrolyte volumes. The costs of the plant increase with its dimension and include the installation of thermal, fluid-dynamic and electric probes, hydraulic system, power conditioning system (PCS), contactors, cables and control panels. The US Department of Energy (DOE) has established cost and performance targets for long-term storage technology systems with the aim of reaching a maximum capital cost (CAPEX) of $150/kWh (≈€150/kWh) with a cycle life of more than 5000 cycles [52]. Nowadays, the capital cost of a VFB is around 600 €/kWh and the Levelized Cost of Storage (LCOS) swings between 0.10 and 0.4 €/kWh [53,54], depending on the ratio Energy to Power [E/P] and on some assumptions made in the analysis. In fact, some studies consider only the costs of stack, reservoir and electrolyte, whereas others include the site construction and the maintenance costs. Poli et al. provide cost analyses which include the entire process, from stack production to the realization of the storage system and its maintenance work [55]. In their analysis CAPEX and LCOS were calculated at different system sizes, assuming 20 years as overall life of the battery, one maintenance intervention every five years and a discount rate of 8%. The results suggest that a VFB systems with E/P higher than 4 h can be profitable, with a Net Present Value (NPV) that can reach the 2 M€ in twenty years when E/P = 10 h (Fig. 10).

Features, advantages, and developments of flow batteries allow to forecast that this technology will expand its penetration in the future. Reducing the costs of active cell materials and electrolytes, which constitute the higher voices of the investment [56,57], as well as moving toward stack with higher power [58], will allow a reduction of the investment costs. It must be considered that the economic return depends on the energy price and if this increase, a higher CAPEX can result in the

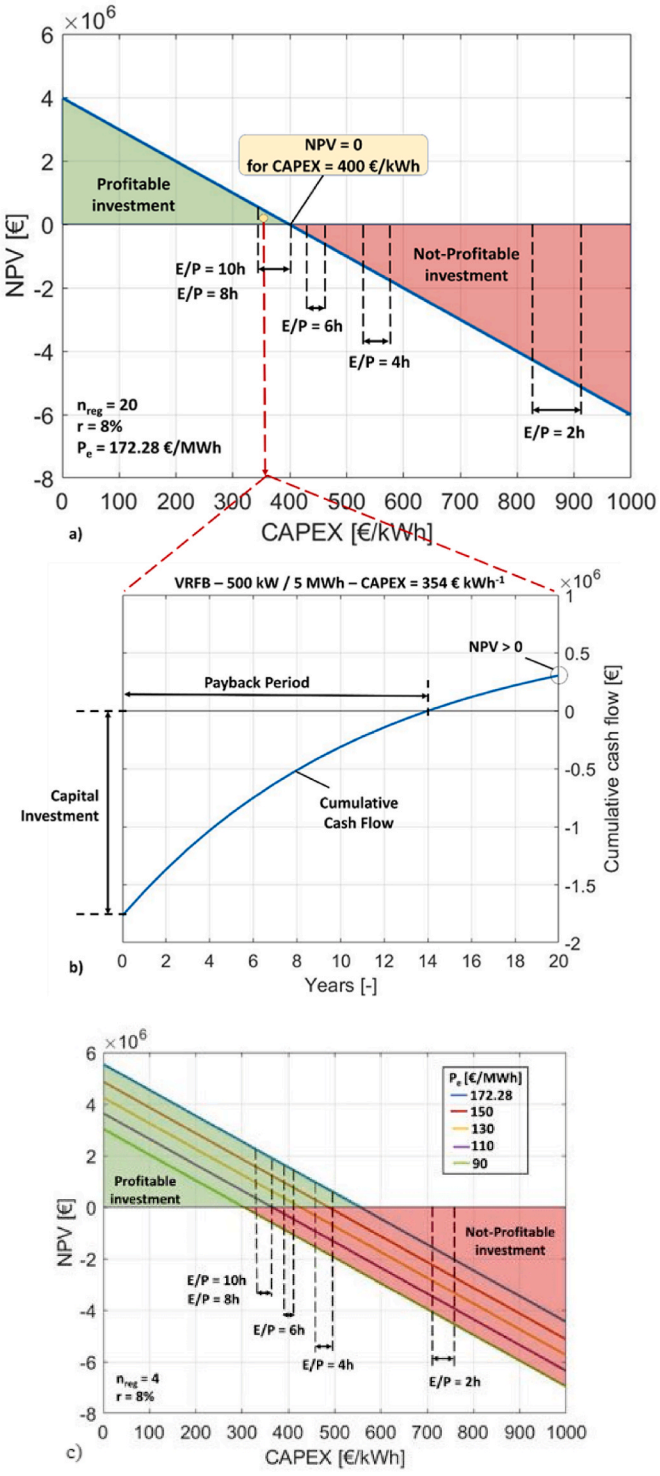

Fig. 10. a) NPV values as a function of CAPEX for VFBs with a duration that varies between 2 and 20 h. b) Cumulative cash flow diagram (CCF) for a VFB system with a E/P ratio of 10 h. c) Variation of the NPV value, as a function of CAPEX, with an annual number of regeneration processes equal to 4 and a discount rate of 8% (E/P ratio between 2 and 10 h) [55].

same break-even point. A major factor that makes this technology competitive is the overall life and a lifetime longer than 20 years, as expected, makes profitable and competitive an investment higher than in other storage technologies.

5. Market perspective and investment strategies

In last two decades, flow batteries have presented a gradual pace of implementation and future projects are expected to gain increased market share. At present some very large plants have been built or are under construction, confirming that VFBs are solutions of choice for large systems thanks to the economies of scale which they feature. The largest project is a 200 MW/800 MWh plant under construction by Rongke Power at Dalian, China [11]. Other examples of plants rated above 1 MW are reported in Table 1.

These projects are evidence of the growing importance of flow batteries globally, notably in large ESSs [60]. A major European manufacturer guarantees 25-years with no degradation on its batteries [61], which is key in enhancing the customer trust in VFB technology. Annual VFB project deployment revenue is projected to grow from $856.4 million in 2022 to $7.76 billion by 2031 [62]. The main barrier to adopt VFB by residential users, in support to photovoltaic panels or mini wind turbines, is the high investment of small VFBs. In the last decades we did not assist to a significant drop in the CAPEX of VFBs, which is set to 500 €/kWh for a 4-h discharge system [55,63], but costs are expected to reduce as the demand expand.

Table 1
World installations of vanadium flow batteries rated above 1 MW.

Producer	Plant/location	Power [MW]	Energy [MWh]	Discharge duration [h]
VRB Energy	Xiangyang, China	100	500	5
Shanghai Electric	Yancheng, China	100	400	4
CellCube	Gonazales, Port Augusta, Australia	50	200	4
Korid Energy	New York, US	50	200	4
Sumitomo	Hokkaido, Japan	17	51	3
Concentric Power	Salinas, California, US	16	128	8
Sumitomo	Abira-Chou, Japan	15	60	4
Shanghai Electric	Xinjiang, China	7.5	22.5	3
Concentric Power	Gonazales, California, US	10	80	8
Rongke Power	Kaifeng, China	6	24	4
Concentric Power	Monterey, California, US	6	18	3
Sumitomo	Tomamae, Japan	6	6	1
H2 Inc	California, US	5	20	4
Rongke Power	Faku, China	5	10	2
VRB Energy	Gonghe, China	3	15	5
VRB Energy	Zaoyang, China	3	12	4
Rongke Power	Jinzhou, China	3	6	2
Enel-Largo	Mallorca, Spain	1.1	5.5	5
VRB Energy	Gonghe, China	2	10	5
Gildemeinster	Milton, Canada	2	8	4
UET	Everett, US	2	8	4
Rongke Power	Snohomish, US	2	8	4
Sumitomo	San Diego, US	2	8	4
Invinity	Yadlamaklka, Australia	2	8	4
VRB Energy	Zhangbei, China	2	8	4
Invinity	Energy Superhub Oxford (ESO) [59]	2	5	2.5
Rongke Power	Jinzhou, China	2	4	2
Rongke Power	Qinghai, China	1	5	5
Shanghai Electric	Qinghai, China	1	5	5
Rongke Power	Washington, US	1	3.2	3.2
Sumitomo	Yokohama, Japan	1	5	5
Bushveld	Brits, South Africa	1	4	4
Rongke Power	Wafangdian, China	1	4	4
Enerox	Mokopane, South Africa	1	4	4
Rongke Power	Tengzhou, China	1	2	2
Shanghai Electric	Shantou, China	1	1	1

A reduction of costs comes from size scaling up and extended discharge duration to 8 h and more, thanks to the lower incidence of the power components, following the demand increase for long duration energy storage. In fact, some of the large project reported above already exceed largely the 4 h duration. VFB stacks are mostly assembled manually at present, at the best of our knowledge, and a major CAPEX decrease can come from robotized production, that can reduce manufacturing and amortization costs to few points percent of raw material costs.

VFBs have reached a technological readiness level (TRL) that qualifies them as reliable and efficient and, also in the framework of the accelerated transition to renewable sources, a fast growth of VFB demand is often forecast. The investment costs of VFB are still higher than Li-ion batteries, which hold the largest share of the stationary storage market. However, if the capacity fade of Li-ion can be recovered adding new battery modules to the ESS, in VFBs it is possible to counteract crossover imbalance and to retrieve the original capacity by simple rebalancing of the electrolytes, which restores the pristine properties of the electrolytes and no spent vanadium issue emerges. As mentioned in Section 4, the mixing procedure can be executed automatically without human supervision or by using alternatively anionic (AEM) and cationic (CEM) exchange membranes in the cells [64–66]. In the latter case, the capacity decay is more than halved and constant capacity can be maintained for more than 200 cycles, so that one balancing procedure per year is sufficient to restore the nominal capacity of the battery. The impact of rebalancing on the LCOS depends on the rebalancing strategy (e.g. rebalancing schedule and lost capacity threshold), technique (e.g. how the rebalancing is obtained: via CEM and AEM or via hydraulic shunt), initial design of the system (type of membrane and battery load) and the investment approach (e.g. electrolyte leasing). In real applications it is important to evaluate how the capital expenditure increases with the frequency of rebalancing [67]. Energy authorities in several countries (e.g. US DOE) state a target lifespan of 5000 cycles for energy storage systems, however many studies and producer datasheets pinpoint a VFB lifespan above 15,000 cycles which provides a much lower need of reinvestment in EES over the years. In fact, long lifespan lowers LCOS making VFB more competitive than other batteries as regards this major key performance indicator.

In addition, long lifespan allows VFBs to be discharged several times each day for short duration services, discharged once in a day for a long service, or some combination of these services. A market boost can also derive from government founding policies. In addition, producers can ease market penetration by offering leasing options of the whole battery or for the electrolytes only to reallocate the cost through a long-term period. Recycling is a key factor to minimize the raw materials demand and promote a circular economy. In the case of VFBs the systems can be recycled almost completely. FF, BP, pipes and tanks, which are made of PP, PE or PVC can be reused [68–70], as well as the heads of the stack made of aluminum or steel and the felts made of carbon. If the system is properly designed the electrolytes at the end of the battery life can be directly used in other VFBs. In the unlike case that electrolytes were contaminated, vanadium can be extracted through precipitation processes and reused in the production of new electrolyte. Alternatively, vanadium can be sold to the iron and steel industry which sums up 80% of the whole vanadium demand, in a market trend where the production of vanadium is constantly increasing, from 35,000 t in 1994 to almost 90,000 t in 2020 [71].

6. Conclusions

Building on the experiences gained at the Electrochemical Energy

Storage and Conversion Lab (EESCoLab) at the University of Padova (Italy) and on pertinent scientific literature, the paper has presented the main features of large-scale all-vanadium flow batteries and their potentials in providing power quality and energy management services for future smart and micro grids applications. The electric, thermal and hydraulic aspects have been outlined with the aim of indicating criteria for the development of competitive VFBs for industrial applications. kW and MW-class VFB have already been manufactured and put into service in different countries, proving their intrinsic safety, long lifetime and full recyclability. Improvements in power and energy density, electrolyte stability and active materials performance and costs, as well developments in engineering features such as mitigation of shunt currents and pumping consumption, will contribute to a larger commercial diffusion of this technology. Processing and manufacturing advancements together with the evolution of the market demand for energy storage are expected to galvanize production and reduce costs, taking the technology to larger and larger market shares.

Declaration of competing interest

The authors declare that they have no known competing financial interests or personal relationships that could have appeared to influence the work reported in this paper.

Acknowledgements

The work was supported by funding from the project “Grid-optimized vanadium redox flow batteries: architecture, interconnection and economic factors” (GUAR-RICERCALASCITOLEVI 20–01) funded by the Interdepartmental Centre Giorgio Levi Cases for Energy Economics and Technology of University of Padua within its 2019 Research Program, from the project “Holistic approach to EneRgy-efficient smart nanO-GRIDS – HEROGRIDS” (PRIN 2017 2017WA5ZT3) within the Italian MUR 2017 PRIN program.

References

[1] The national academies summit on America’s energy future: summary of a meeting, N. R. C. Committee for the National Academies Summit on America’s Energy Future, National Academies Press, Washington, DC, 2008.
[2] E. Reihani, M. Motalleb, R. Ghorbani, L.S. Saoud, Load peak shaving and power smoothing of a distribution grid with high renewable energy penetration, Renew. Energy 86 (2016) 1372–1379.
[3] S. Rehman, L.M. Al-Hadhrami M.M. Alam, Pumped hydro energy storage system: a technological review, Renew. Sustain. Energy Rev. 44 (2015) 586–598.
[4] A.G. Olabi, T. Wilberforce, M. Ramadan, M. Ali Abdelkareem, A.H. Alami, Compressed air energy storage systems: components and operating parameters – a review, J. Energy Storage 34 (2021), 102000.
[5] H. Zhang, J. Baeyens, G. Cáceres, J. Degrève, Y. Lv, Thermal energy storage: recent developments and practical aspects, Prog. Energy Combust. Sci. 53 (2016) 1–40.
[6] A.G. Olabi, T. Wilberforce, M.A. Abdelkareem, M. Ramadan, Critical review of flywheel energy storage system, Energies 14 (2020) 2159.
[7] V.S. Vulusala, S. Madichetty, Application of superconducting magnetic energy storage in electrical power and energy systems: a review, Int. J. Energy Res. 42 (2018) 358–368.
[8] B.H. Li, X.S. Pan, Y.B. He, H.D. Du, Study of EDLC and its usage in stand-alone photovoltaic system, Adv. Mater. Res. 335 – 336 (2011) 1368–1375.
[9] E. Sanchez-Díez, E. Ventosa, M. Guarnieri, A. Trovò, C. Flox, R. Marcilla, F. Soavi, Petr Mazur, E. Aranzabe, R. Ferret, Redox flow batteries: status and perspective towards sustainable stationary energy storage, J. Power Sources 481 (2021), 228804.
[10] A. Khor, P. Leung, M. Mohamed, C. Flox, Q. Xu, L. An, R. Wills, J. Morante, A. Shah, Review of zinc-based hybrid flow batteries: from fundamentals to applications, Mater. Today Energy 8 (2018) 80–108.
[11] Energy Storage News, First phase of 800MWh world biggest flow battery commissioned in China. https://www.energy-storage.news/first-phase-of-800mwh-world-biggest-flow-battery-commissioned-in-china. (Accessed 22 December 2022) accessed.
[12] S. Roe, C. Menictas, M. Skyllas-Kazacos, A high energy density vanadium redox flow battery with 3 M vanadium electrolyte, J. Electrochem. Soc. 163 (2016) A5023–A5028.
[13] K. Knehr, E. Kumbur, Open circuit voltage of vanadium redox flow batteries: discrepancy between models and experiments, Electrochem. Commun. 13 (4) (2011) 342–345.
[14] M. Guarnieri, A. Trovò, A. D’Anzi, P. Alotto, Developing vanadium redox flow technology on a 9-kW 26-kWh industrial scale test facility: design review and early experiments, Appl. Energy 230 (2018) 1425–1434.
[15] C. Jia, J. Liu, C. Yan, A multilayered membrane for vanadium redox flow battery, J. Power Sources 203 (2012) 190–194.
[16] C. Jia, J. Liu, C. Yan, A significantly improved membrane for vanadium redox flow battery, J. Power Sources 195 (2010) 4380–4383.
[17] Q. Luo, H. Zhang, J. Chen, D. You, C. Sun, Y. Zhang, Preparation and characterization of Nafion/SPEEK layered composite membrane and its application in vanadium redox flow battery, J. Membr. Sci. 325 (2008) 553–558.
[18] M. Yue, Y. Zhang, L. Wang, Sulfonated polyimide/chitosan composite membrane for vanadium redox flow battery: membrane preparation, characterization, and single cell performance, J. Appl. Polym. Sci. 127 (2013) 4150–4159.
[19] A. Di Blasi, N. Briguglio, O. Di Blasi, V. Antonucci, Charge–discharge performance of carbon fiber-based electrodes in single cell and short stack for vanadium redox flow battery, Appl. Energy 125 (2014) 114–122.
[20] J. Sun, L. Zeng, H.R. Jiang, C.Y.H. Chao, T.S. Zhao, Formation of electrodes by self-assembling porous carbon fibers into bundles for vanadium redox flow batteries, J. Power Sources 405 (2018) 106–113.
[21] A. Di Blasi, O. Di Blasi, N. Briguglio, A.S. Aricò, D. Sebastián, M.J. Lázaro, G. Monforte, V. Antonucci, Investigation of several graphite-based electrodes for vanadium redox flow cell, J. Power Sources 227 (2013) 15–23.
[22] J. Zhang, T. Zhou, L. Xia, C. Yuan, W. Zhang, A. Zhang, Polypropylene elastomer composite for the all-vanadium redox flow battery: current collector materials, J. Mater. Chem. 3 (2015) 2387–2398.
[23] L. Dongyoung, C. Jaeheon, N. Soohyun, L. Jun Woo, C. Ilbeom, L. Dai Gil, Development of non-woven carbon felt composite bipolar plates using the soft layer method, Compos. Struct. 160 (2017) 976–982.
[24] K. Kyungmun, P. Sunghyun, J. Ahrae, L. Kise, J. Hyunchul, Development of ultralight and thin bipolar plates using epoxy-carbon fiber prepregs and graphite composites, Int. J. Hydrogen Energy 42 (2017) 1691–1697.
[25] C. Jaeheon, L. Jun Woo, K. Minkook, K. Jinwhan, L. Dai Gil, Durability of graphite coated carbon composite bipolar plates for vanadium redox flow batteries, Compos. Struct. 134 (2015) 106–113.
[26] S. Nam, D. Lee, J. Kim, D.G. Lee, Development of a fluoroelastomer/glass fiber composite flow frame for a vanadium redox flow battery (VFB), Compos. Struct. 145 (2016) 113–118.
[27] M. Guarnieri, A. Trovò, G. Marini, A. Sutto, P. Alotto, High current polarization tests on a 9 kW vanadium redox flow battery, J. Power Sources 431 (2019) 239–249.
[28] A. Trovò, M. Guarnieri, Battery management system with testing protocols for kW-class vanadium redox flow batteries, in: 2020 2nd IEEE International Conference on Industrial Electronics for Sustainable Energy Systems (IESES), 2020.
[29] A. Trovò, V. Di Noto, J.E. Mengou, C. Gamabaro, M. Guarnieri, Fast response of kW-class vanadium redox flow batteries, IEEE Trans. Sustain. Energy 12 (4) (2021) 2413–2422.
[30] A.A. Kurilovich, A. Trovò, M. Pugach, K.J. Stevenson, M. Guarnieri, in: Prospect of Modeling Industrial Scale Flow Batteries – from Experimental Data to Accurate Overpotential Identification, vol. 167, 2022, 112559.
[31] C. Zhang, T.S. Zhao, Q. Xu, L. An, G. Zhao, Effects of operating temperature on the performance of vanadium redox flow batteries, Appl. Energy 155 (2015) 349–353.
[32] A. Fetyan, G.A. El-Nagar, I. Lauermann, M. Schnucklake, J. Schneider, C. Roth, Detrimental role of hydrogen evolution and its temperature-dependent impact on the performance of vanadium redox flow batteries, J. Energy Chem. 32 (2019) 57–62.
[33] H. Al-Fetlawi, A.A. Shah, F.C. Walsh, Modelling the effects of oxygen evolution in the all-vanadium redox flow battery, Electrochim. Acta 55 (2010) 3192–3205.
[34] J. Zhang, L. Li, Z. Nie, B. Chen, M. Vijayakumar, S. Kim, W. Wang, B. Schwenzer, J. Liu, Z. Yang, Effects of additives on the stability of electrolytes for all-vanadium redox flow batteries, J. Appl. Electrochem. 41 (2011) 1215–1221.
[35] M. Skyllas-Kazacos, C. Menictas, M. Kazacos, Thermal stability of concentrated V (V) electrolytes in the vanadium redox cell, J. Electrochem. Soc. 143 (1996) L86.
[36] L. Li, S. Kim, W. Wang, M. Vijayakumar, Z. Nie, B. Chen, J. Zhang, G. Xia, J. Hu, G. Graff, J. Liu, Z. Yang, A stable vanadium redox-flow battery with high energy density for large-scale energy storage, Adv. Energy Mater. 1 (2011) 394–400.
[37] S. Li, K. Huang, S. Liu, D. Fang, X. Wu, D. Lu, T. Wu, Effect of organic additives on positive electrolyte for vanadium redox battery, Electrochim. Acta 56 (2011) 5483–5487.
[38] M. Ding, T. Liu, Y. Zhang, Z. Cai, Y. Yang, Y. Yuan. Effect of Fe (III) on the positive electrolyte for vanadium redox flow battery. R. Soc. Open Sci. 6: 181309.
[39] A. Trovò, P. Alotto, M. Giomo, F. Moro, M. Guarnieri, A validated dynamical model of a kW-class Vanadium Redox Flow Battery, Math. Comput. Simulat. 183 (2021) 66–77.
[40] A. Trovò, M. Guarnieri, Standby thermal management system for a kW-class vanadium redox flow battery, Energy Convers. Manag. 226 (2020), 113510.
[41] A. Tang, J. Bao, M. Skyllas-Kazacos, Studies on pressure losses and flow rate optimization in vanadium redox flow battery, J. Power Sources 248 (2014) 154–162.
[42] A. Trovo, F. Picano, M. Guarnieri, Comparison of energy losses in a 9 kW vanadium redox flow battery, J. Power Sources 440 (2019), 227144.
[43] C. Choi, S. Kim, R. Kim, Y. Choi, S. Kim, H. Jung, J.H. Yang, H. Kim, A review of vanadium electrolytes for vanadium redox flow batteries, Renew. Sustain. Energy Rev. 69 (2017) 263–274.
[44] L. Mou, M. Huang, A.P. Klassen, M.A.M. Harper, in: Redox Flow Battery and Method for Operating the Battery Continuously in a Long Period of Time. Patent No.: US 10,608,274 B2, 2020. Date of patent: Mar. 31.

[45] N. Poli, M. Schäffer, A. Trovò, J. Noack, M. Guarnieri, P. Fischer, Novel electrolyte rebalancing method for vanadium redox flow batteries, Chem. Eng. J. 405 (2021), 126583.
[46] I. Derr, D. Przyrembel, J. Schweer, A. Fetyan, J. Langner, J. Melke, M. Weinelt, C. Roth, Electroless chemical aging of carbon felt electrodes for the all-vanadium redox flow battery (VFB) investigated by Electrochemical Impedance and X-ray Photoelectron Spectroscopy, Electrochim. Acta 246 (2017) 783–793.
[47] K.H. Kim, B.G. Kim, D.G. Lee, Development of carbon composite bipolar plate (BP) for vanadium redox flow battery (VFB), Compos. Struct. 109 (2014) 253–259.
[48] A. Trovò, W. Zamboni, M. Guarnieri, Multichannel Electrochemical Impedance Spectroscopy and equivalent circuit synthesis of a large-scale vanadium redox flow battery, J. Power Sources 493 (2021), 229703.
[49] H.S. Magar, R.Y.A. Hassan, A. Mulchandani, Electrochemical impedance spectroscopy (EIS): principles, construction, and biosensing applications, Sensors 21 (19) (2021) 6578.
[50] J. Gouveia, A. Mendes, R. Monteiro, T.M. Mata, N.S. Caetano, A.A. Martins, Life cycle assessment of a vanadium flow battery, Energy Rep. 6 (2020) 95–101.
[51] A. Tang, J. McCann, J. Bao, M. Skyllas-Kazacos, Investigation of the effect of shunt current on battery efficiency and stack temperature in vanadium redox flow battery, J. Power Sources 242 (2013) 349–356.
[52] US Department of Energy, Grid energy storage. https://www.energy.gov/sites/prod/files/2014/09/f18/Grid%20Energy%20Storage%20December%202013.pdf.
[53] C. Minke, T. Turek, Material, system designs and modelling approaches in techno-economic assessment of all-vanadium redox flow batteries, J. Power Sources 376 (2018) 66–81.
[54] M.J. Li, W. Zhao, X. Chen, W.Q. Tao, Economic analysis of a new class of vanadium redox-flow battery for medium- and large-scale energy storage in commercial applications with renewable energy, Appl. Therm. Eng. 114 (2017) 802–814.
[55] N. Poli, C. Bonaldo, A. Trovò, M. Moretto, M. Guarnieri. Techno-economic Assessments of Vanadium Flow Batteries: Performance and Value Analysis. Applied Energy, *(Under revision)*.
[56] M. Zhang, M. Moore, J.S. Watson, T.A. Zawodzinski, R.M. Counce, Capital cost sensitivity analysis of an all-vanadium redox-flow battery, J. Electrochem. Soc. 159 (8) (2012) A1183–A1188.
[57] C. Minke, T. Turek, Economics of vanadium redox flow battery membranes, J. Power Sources 361 (2017) 105–114.
[58] C. Minke, U. Kunz, T. Turek, Techno-economic assessment of novel vanadium redox flow batteries with large-area cells, J. Power Sources 361 (2017) 105–114.
[59] Energy Superhub Oxford, Official website. https://energysuperhuboxford.org/. (Accessed 22 December 2022) accessed.
[60] Worldwide installations of vanadium flow batteries (VFBs), Vanitec official website, https://vanitec.org/vanadium/map. (Accessed 22 December 2022). accessed.
[61] Service and guarantee offered by the company CellCube, CellCube official website, https://www.cellcube.com/service-and-guarantee/. (Accessed 22 December 2022). accessed.
[62] Vanadium flow battery: identifying market opportunities and enablers, Vanitec official website, https://vanitec.org/images/uploads/Guidehouse_Insights-Vanadium_Redox_Flow_Batteries. pdf. (Accessed 22 December 2022). accessed.
[63] V. Viswanathan, A. Crawford, D. Stephenson, S. Kim, W. Wang, B. Li, G. Coffey, E. Thomsen, G. Graff, P. Balducci, M. Kintner-Meyer, V. Sprenkle, Cost and performance model for redox flow batteries, J. Power Sources 247 (2014) 1040–1051.
[64] A. Bhattarai, P.C. Ghimire, A. Whitehead, R. Schweiss, G.G. Scherer, N. Wai, H. H. Hng, Novel approaches for solving the capacity fade problem during operation of a vanadium redox flow battery, Batteries 4 (2018) 48.
[65] K. Wang, L. Liu, J. Xi, Z. Wu, X. Qiu, Reduction of capacity decay in vanadium flow batteries by an electrolyte-reflow method, J. Power Sources 338 (2017) 17–25.
[66] A. Bhattarai, N. Wai, R. Schweiss, A. Whitehead, G.G. Scherer, P.C. Ghimire, T. M. Lim, H.H. Hng, Vanadium redox flow battery with slotted porous electrodes and automatic rebalancing demonstrated on a 1 kW system level, Appl. Energy 236 (2019) 437–443.
[67] N. Poli, A. Trovò, P. Fischer, J. Noack, M. Guarnieri, Electrochemical Rebalancing Process for Vanadium Flow Batteries: Sizing and Economic Assessment, J. Energy Storage 58 (2023) 106404.
[68] J.C. Lee, Kurniawan, E.Y. Kim, K.W. Chung, R. Kim, H.S. Jeon, A review on the metallurgical recycling of vanadium from slags: towards a sustainable vanadium production, J. Mater. Res. Technol. 12 (2021) 343–364.
[69] D. Jubinville, E. Esmizadeh, S. Saikrishnan, C. Tzoganakis, T. Mekonnen, A comprehensive review of global production and recycling methods of polyolefin (PO) based products and their post-recycling applications, Sustainable Materials and Technologies 25 (2020), e00188.
[70] K. Lewandowski, K. Skórczewska, A brief review of poly (vinyl chloride) (PVC) recycling, Polymers 14 (2022) 3035.
[71] G.J. Simandl, S. Paradis, Vanadium as a critical material: economic geology with emphasis on market and the main deposit types, B. Appl. Earth Sci. 131 (4) (2022) 218–236.